TEST TECHNIQUES

Karl-Heinz Schwalbe,
GKSS Research Centre Geesthacht,
2054 Geesthacht,
West-Germany

ABSTRACT

Test methods for fracture mechanics tests are described. Two groups of techniques are distinguished: Those for measurement of stable crack growth and those for determination of the loading parameters.

KEY WORDS

Test methods; stable crack growth; initiation of growth; compliance; electrical potential; load interruption; caustics; crack tip opening displacement; infiltration method.

BACKGROUND

The theme "Techniques for Fracture Testing" covers a very large area and it is impossible to treat all subjects of interest within a 30 minutes presentation. It is therefore intended to concentrate upon fracture mechanics testing only and within this area upon the most important problems. It is not the intention of the present paper to describe standardized test procedures in detail but to give a survey on both widely used and less common techniques.

The test techniques that have to be applied depend on the problem to be solved. In the following, some test procedures and their application will be discussed by means of Eq(1)

$$\Delta a,\ \frac{da}{dN},\frac{da}{dt},\ = f(K,J,\text{ or }\delta) \qquad (1)$$

which represents the most important test task in fracture mechanics: *determination of crack growth as a function of a loading parameter*. The determination of *initiation* of crack growth is only a special case of that problem: initiation is determined by back-extrapolation of growth data to zero growth.

The left hand side of Eq(1) represents crack growth as the material's response to loading; this will be the subject of paragraph 2. The right hand side will be discussed in paragraph 3. Whereas K, J, δ are material independent loading parameters, their critical values K_o, J_o, δ_o or K_c, J_c, δ_c are material properties which indicate the onset of stable crack growth and instability in load controlled situations, respectively. Fig. 1 shows a survey on the parameters and their experimental determination.

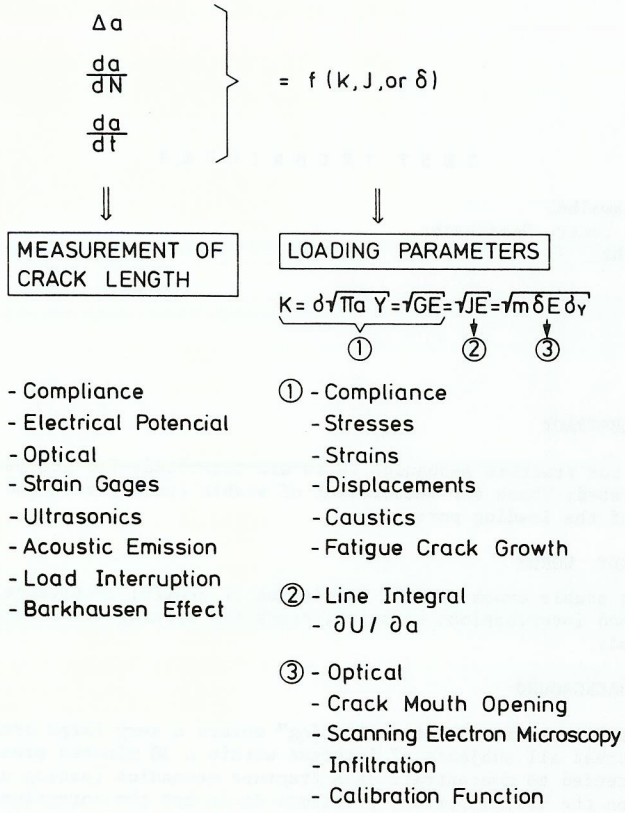

Fig. 1: Survey on the experimental determination of the parameters discussed in the present paper

CRACK LENGTH

Optical Methods

The simplest way to measure the length of a crack is by optical observation. The advantage is that "one sees what one measures". Disadvantages are:

- In the case of non-transparent materials only the surface trace of the crack can be observed and measured. In thick specimens - particularly in those subjected to to monotonic loading - this may give a poor impression about what is really happening, since pronounced crack front tunneling may occur, Fig. 2. When the specimen is thin and loaded cyclically the error introduced thereby is small, Fig. 2. Therefore, the optical method is proposed by the ASTM Tentative Test Method for Fatigue Crack Growth (1979).

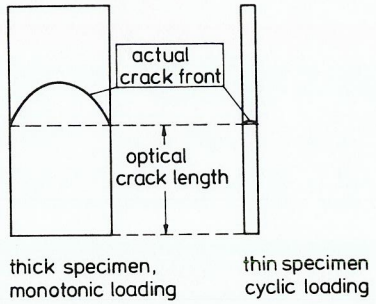

Fig. 2: Crack front behaviour depending on specimen thickness and loading type

- The specimen must be prepared in order to make the crack visible. This is done by polishing that part of the specimen surface the crack is expected to grow through. The measurement itself can be carried out using a travelling microscope and by either counting reference marks applied to the specimen surface (scratch marks, photographic grids etc.) or coupling the microscope with a precision scale or an LVDT.

- The discountinous nature of the optical measurement is a poor prerequisite for automated data recording.

Compliance Method

Fracture mechanics test set ups are in most cases instrumented with a device for the determination of the specimen's compliance. Usually, not the total compliance across the loading points but the compliance across the crack mouth is determined.

The specimen is regarded as a spring whose compliance 2v/F increases with increasing crack length, Fig. 3a. In order the exclude the influence of thickness and elastic properties the compliance is normalised by thickness, B, and Young's modulus, E, Fig. 3b.

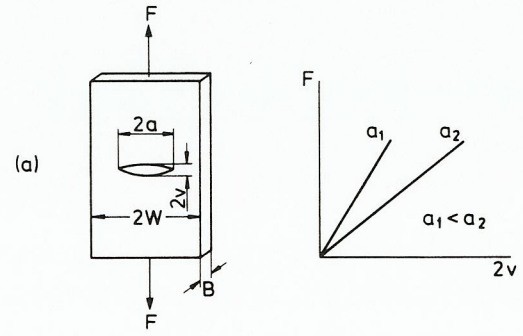

Fig. 3a: Generation of a compliance calibration curve

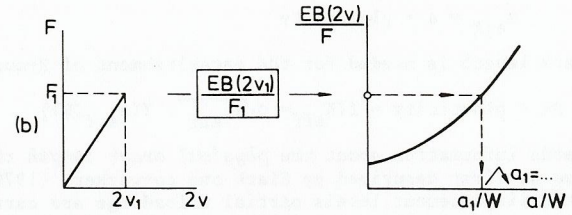

Fig. 3b: Generation of a compliance calibration curve

The influence of specimen width and crack length is excluded by regarding the normalized compliance as a function of the relative crack length, a/W. Thus, the relation

$$\frac{EB(2v)}{F} = f(a/W) \qquad (2)$$

is a compliance calibration depending on the in-plane shape of the specimen only.

Fig. 4 shows an example.

Experimentally determined calibration curves in the form of Eq(2) can be used to obtain actual crack lengths during a fracture mechanics test. However, more convenient and more straightforward with respect to computer aided data recording and data reduction is the application of analytical calibration curves. For centre cracked panels Eftis and Liebowitz (1972) obtained:

$$\frac{EB(2v)}{F} = \sqrt{\frac{\pi a}{2W}\Big/\sin\frac{\pi a}{2W}} \left\{ \frac{4W}{\pi y} \operatorname{arcosh} \left[\frac{\cosh\frac{\pi y}{2W}}{\cos\frac{\pi a}{2W}} \left[1 + \left\{ \frac{\sin\frac{\pi a}{2W}}{\sinh\frac{\pi a}{2W}} \right\}^2 \right]^{-\frac{1+\nu}{0,5}} \right] + \nu \right\} \frac{y}{W} \qquad (3a)$$

$$0.2 < \frac{a}{W} < 0.8; \quad \frac{y}{W} \leq 0.5$$

2y: span of gage
2v: crack opening displacement at centre line of specimen.

Fig. 5 shows a comparison with experimental results (Schwalbe and Setz). Saxena and Hudak (1978) found for the compact specimen

$$\frac{EB(2v)}{F} = \left[1 + \frac{0.25}{a/W}\right]\left[\frac{1+a/W}{1-a/W}\right]^2 \Big\{ 1.6137 + 12.6778(a/W) - 14.2311(a/W)^2 - 16.6102(a/W)^3 + 35.0499(a/W)^4 - 14.4943(a/W)^5 \Big\} \qquad (3b)$$

Here 2v is the crack opening displacement at the front face of the specimen.

The relations:

$$\frac{EB(2v)}{F} = -15.37 + 212.95(a/W) - 625.59(a/W)^2 + 825.53(a/W)^3 \qquad (3c)$$

$$0.2 \leq \frac{a}{W} \leq 0.63$$

$$\frac{EB(2v)}{F} = -25707.041 + 113938.914(a/W) - 168567.84(a/W)^2 + 83612.684(a/W)^3 \qquad (3d)$$

$$0.63 \leq a/W \leq 0.88$$

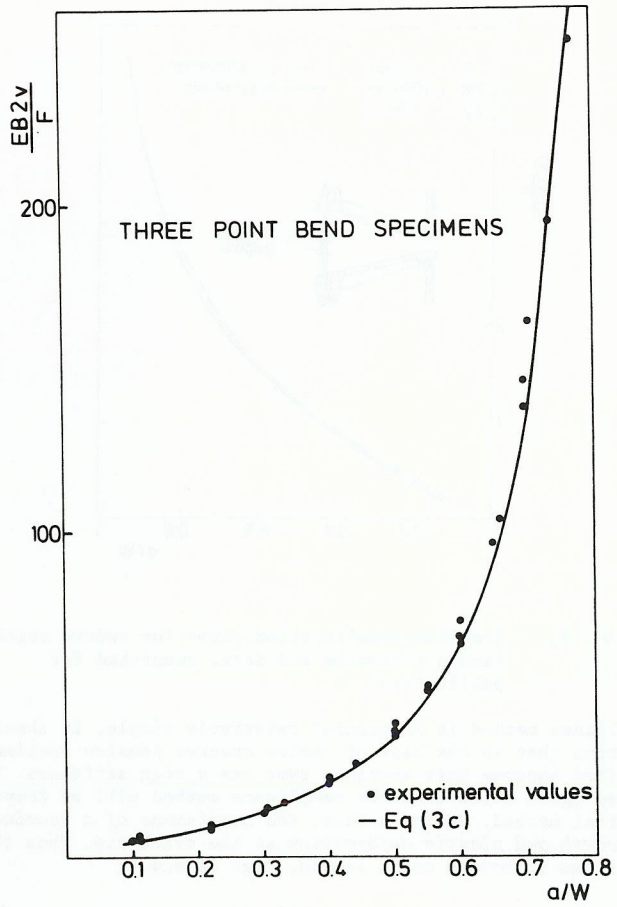

Fig. 4: Compliance calibration for three point bend specimens. The experimental data were obtained on specimens with different thickness, width and modulus of elasticity, Hellmann (1980)

represent a fit of experimented data obtained on three-point-bend specimens (Hellmann 1980), see Fig. 4).

The crack opening displacement is measured using a clip gage which is attached to the specimen by srewed-on or integral knife edges. For centre cracked tension specimens a special arrangement has been developped combining the solution of Sullivan and Stoop (1974) with the advantage of knife edges: at the centre of the specimen a hole is drilled such that a circular knife edge results in the specimen's mid-plane. The radius of the ends of the clip gage is slightly smaller than that of the knife edge.

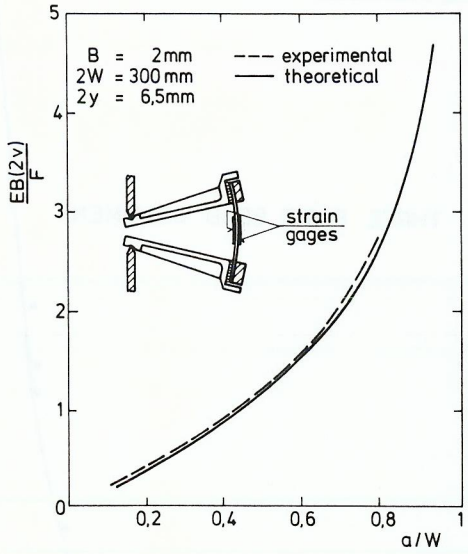

Fig. 5: Compliance calibration curve for centre cracked panels (Schwalbe and Setz, submitted for publication).

While the compliance method is in general relatively simple, it should be taken into consideration that in the case of centre cracked tension specimens high precision is required because this specimen type has a high stiffness. This problem will be stressed again below when the compliance method will be compared with the electric potential method. During a test, *the compliance of a specimen increases due to crack growth and plastic deformation* at the crack tip. Thus the compliance method measures an *effective crack length*, Fig. 6a and b:

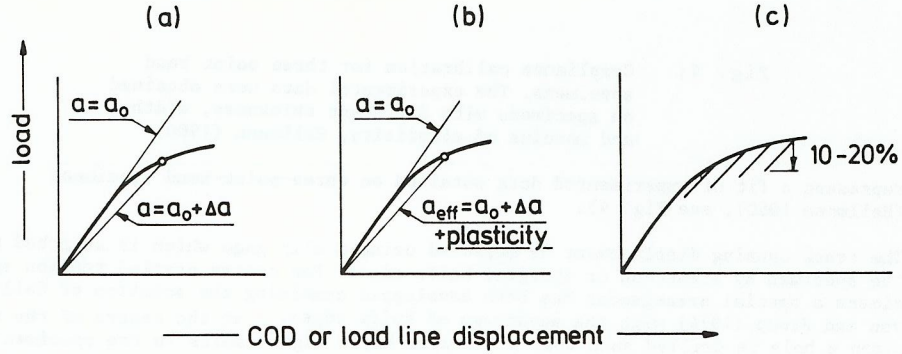

Fig. 6a and 6b: Determination of effektive and physical crack length from compliance measurements.

$$a_{eff} = a + \text{plasticity} \quad (4)$$

This effective crack length is needed for the establishment of R-curves

$$\Delta a_{eff} = \Delta a + \text{plasticity} = f(K_{eff} = \sigma\sqrt{\pi a_{eff}} \cdot Y(a_{eff}/W)) \quad (5)$$

However, if one needs information about the *physical crack length* the *partial unloading technique* as first described by Clark and co-workers (1976) can be applied. At selected displacement levels partial unloadings are carried out; the unloading slope represents the elastic compliance of the specimen and is therefore representative for the actual physical crack length, Fig. 7c. The partial unloading technique requires high precision of experimental work; particularly friction effects (bolts/specimen; clip gage/knife-edges) must be eliminated.

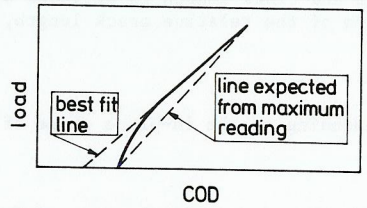

Fig. 7: Interpretations of a nonlinear load-COD record, Sullivan (1975).

When tracking fatigue crack growth special attention should be directed to initial nonlinearities of the load/COD records. From linear elastic considerations a strictly linear record is expected as long as the maximum fatigue load meets the conditions for linear elastic fracture mechanics. Thus, maximum readings for load and COD are expected to give the informations required for the slope determination. However, as Fig. 7 shows, initial nonlinearities which are caused by crack closure would give rise to incorrect conclusions. It is therefore advisable to construct a straight line as demonstrated in Fig. 7 (Sullivan, 1975).

Potential Method

An elegant method for crack length measurement is provided by the electric potential field built up in a specimen which is connected to current leads. In principle both direct and alternating current are applicable; however, mostly DC is preferred to avoid any detrimental effects which may arise due to the current gradients with respect to time.

The application of the potential method has been investigated experimentally and theoretically by examining a number of current and potential lead positions and specimen geometries (Aronson and Ritchie, 1979; Clark and Knott, 1975; Gilby and Pearson, 1966; Johnson, 1965; Ritchie and Bathe, 1979; Rooke, 1967; Russenberger, 1979; Schwalbe and Hellmann, submitted for publication; Srawley and Brown, 1965).

The sensitivity of the potenial method depends strongly on the location of the leads for current and potential respectively. Fig. 8 shows for CCT specimens that *the sensitivity is the greater the closer to the crack tip the potential probes are placed.* This effect is demonstrated more clearly by Fig. 9. For practical applications it is important to note that due to the levelling-off effect for probe positions close to the crack plane very small errors due to misplaced potential probes can be expected.

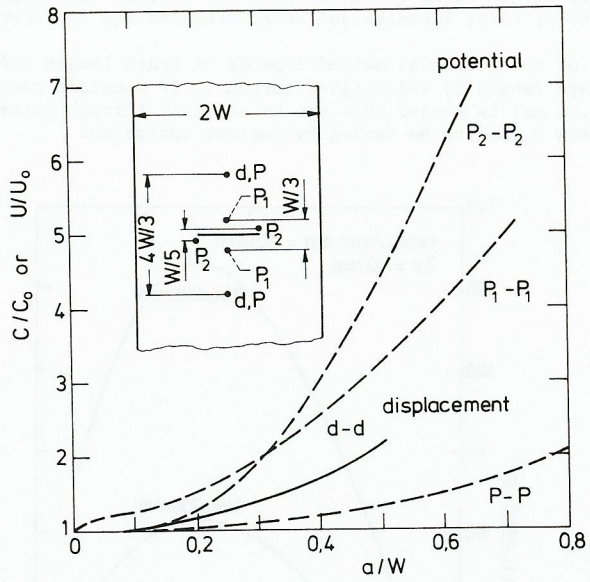

Fig. 8: Potential and compliance calibration for centre cracked panels (Srawley and Brown, 1965).

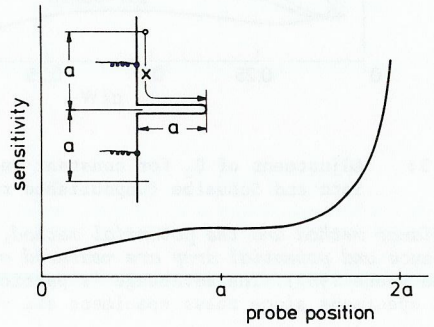

Fig. 9: Sensitivity of the potential method as a function of the probe position (after Clark and Knott, 1975).

On the other hand, close to the crack tip the method is very sensitive but reproducibility is poor since the sensitivity varies strongly with the probe position. Three configurations for CT specimens are shown in Fig. 10a. From the calibration curves it can be seen that configuration 3 is the most sensitive one, Fig. 10b.

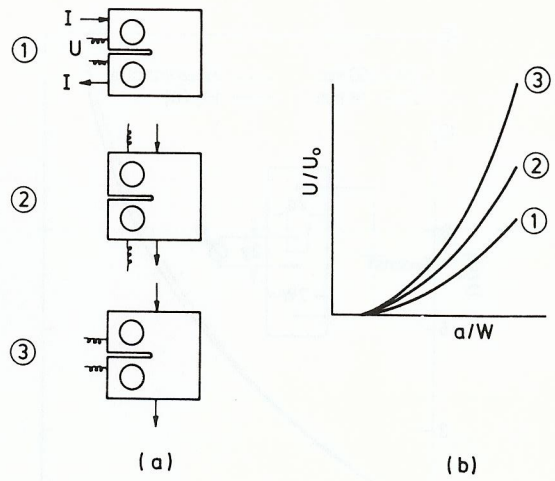

Fig. 10: Three configurations of current and potential locations and their sensitivity (after Aronson and Ritchie, 1979).

These findings suggest that the application of the potential method using the configuration and analytical calibration curve described by Johnson (1965) represents a good compromise between accuracy and ease of application. Johnson considered a centre cracked panel with homogeneous current density over cross sections remote from the crack plane. Starting with an initial crack length a_o which exhibits a potential drop U_o the actual crack length a is given by the actual potential drop U, the specimen width 2W and the gage span 2y for the potential measurement in the following way:

$$a = \frac{2W}{\pi} \arccos \frac{\cosh \frac{\pi y}{2W}}{\cosh \left[\frac{U}{U_o} \operatorname{arcosh} \frac{\cosh \frac{\pi y}{2W}}{\cos \frac{\pi a_o}{2W}} \right]} \qquad (6)$$

The relation is valid for potential probe locations placed symmetrically as shown in Fig. 11. Also shown in Fig. 11 are the theoretical and experimental calibration curves. This way of applying the potential method has the following advantages:

- It is insensitive with respect to misplacement of the potential probes (see Fig. 9).
- The configuration has reasonable sensitivity (see Fig. 8 and 9).
- Application is convenient as data reduction can be done by means of the analytical relationship Eq.(6) which exhibits good agreement with experimental results (see Fig. 11). Furthermore, computer aided data recording and data reduction is facilitated.
- Eq.(6) provides a *calibration which is independent of material, specimen thickness, and current* through the use of the normalized potential U/U_o.
- Normalization with respect to initial state (a_o/U_o) allows precise determination of small crack length increments.

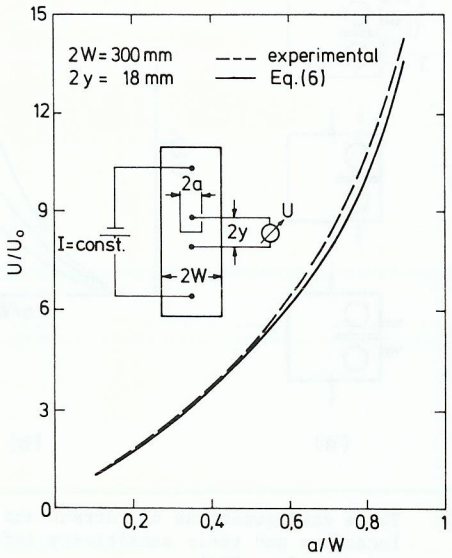

Fig. 11: Experimental and theoretical potential calibration curve for centre cracked panels, Schwalbe and Setz (submitted for publication).

- A further benefit of Eq.(6) is that it can be applied to several specimen geometries (Schwalbe and Hellmann), Fig. 12. These geometries are electrically equivalent although their mechanical behaviour is quite different.

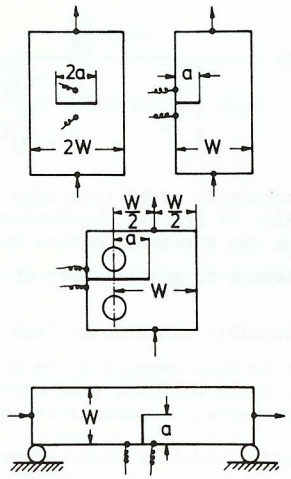

Fig. 12: Specimen geometries which can be treated with Eq(6)

The usefulnes of Eq.(6) could be demonstrated by several investigations (Schwalbe, 1972, 1977a, 1977b, 1979; Schwalbe and Setz; Schwalbe and coworkers).

The resolution of the potential method depends on crack length and specimen width (for a given gage length 2y and a given current). If constant resolution (for example Δa = 0.01 mm) is needed this can be achieved through current adjustment. Fig. 13 shows how U_o has to be varied by current variation.

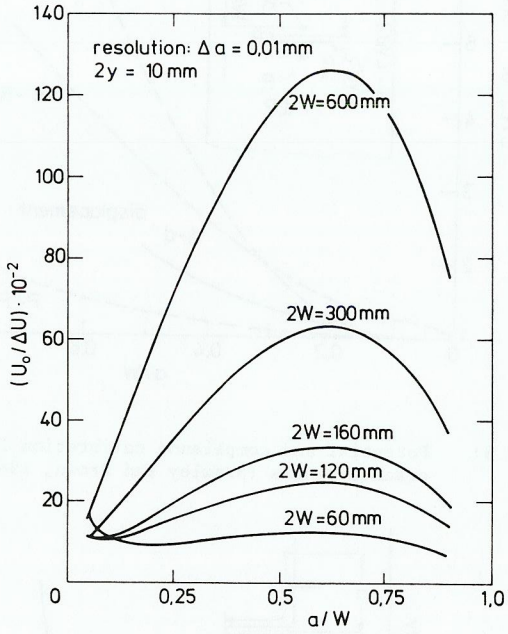

Fig. 13: Adjustment of U_o for constant resolution, Setz and Schwalbe (unpublished results).

Comparing the compliance method and the potential method, the former one is more sensitive if compliance and potential drop are measured over the same gage span, see Fig. 8 (see also Rooke 1967). The advantage is particularly great in the case of compact and bend specimens since these specimens are very compliant.

Nevertheless, the potential method is very useful as it yields direct information about the physical crack length and at least in the case of CCT specimens much less scatter is obtained with the potential method than with the compliance method (Schwalbe and Setz). The reason is that CCT specimens are relatively stiff and it is difficult to measure very small displacements accurately.

Another variant of the potential method works with foils attached to the side surface of the specimen (Russenberger, 1979). It is assumed that the crack running in the specimen underneath the foil causes a crack in the foil of the same length. Advantages are:
- Application of the potential method to non-conducting materials.
- Linear relationship between crack length and potential.

- Due to the high resistance ot the thin foil low amplification is required.

A negative aspect is that this is a surface measurement, so that no information is obtained about the crack behaviour in the interior of the specimen.

Other Methods

The most precise method for crack length measurement is the *load interruption technique*. A number of identical specimens are loaded up to different load levels, unloaded and subsequently fatigued or (in the case of steels with a ductile-brittle transition) broken in liquid nitrogen. If stable crack growth had occured it is visible on the fracture surface; very small amounts of growth can be resolved by the scanning electron microscope. However, since crack growth is very inhomogenous on a microscopic scale measurements have to be made at several equidistant locations along the crack front, Fig. 14. To avoid arbitrary pick up of special features along the crack front it is advisable to make several individual measurements at each location, again at equidistant points Fig. 15. The load interruption techniques is frequently used to calibrate indirect methods.

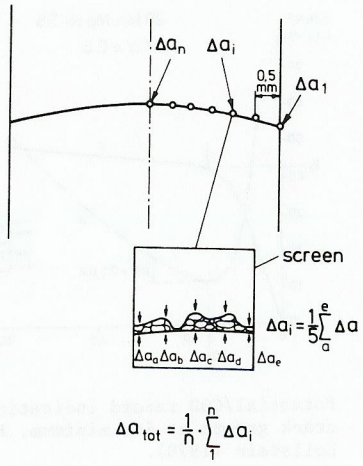

Fig. 14 Determination of average crack growth by scanning electron microscopy, Schwalbe (1974)

Quite similar to this technique is the *heat tinting* method; the specimens which have been loaded to a predetermined load level are unloaded and heated to a temperature which leads to a coloured oxide film on the fracture surface. Subsequent fracturing in liquid nitrogen or by fatigue reveals the position the crack front has reached under the static load.

The methods described above represent standard methods for laboratory use. There are a number of additional methods which are only occasionally used.

Although *ultrasonics* have become an importand tool for in-service inspection of structures (see for example Rose and Rogovsky, 1978) application for crack length measurements in the laboratory is limited. The onset of stable crack growth can be detected with a resolution of $\Delta a \simeq 0.1$ mm (Clark, 1968; Klima, Fisher and Buzzard, 1976). A technique for fatigue crack growth tracking has been developped by Greenberg and co-workers (1969): it involves a stepping motor moving the probe to keep the signal reflected by the crack face constant.

Acoustic emission caused by plastic defomation of the crack tip can be used to determine the crack length (Dunegan and Harris, 1967). Plastic deformation and hence emission are a function of the stress intensity. If the applied load and the K calibration are known the crack length can be determined via experimental calibration. However, acoustic emission provides far less precise informations about the crack length than many other methods. On the other hand, dormant periods of crack growth and that part of the load cycle where growth occurs can be readily observed by this technique (Hartbower and co-workers, 1973). An important field of application of acoustic emission is the in-service survey of structures. A comprehensive survey on the acoustic emission technique is given by ASTM (1972).

Bhattarchaya and Schroeder (1975) make use of the *Barkhausen effect* to measure crack growth in ferromagnetic materials. Fast crack growth steps produce magnetization changes in magnetic domains of the specimen which lead to voltage pulses in a pick up coil surrounding the specimen. The Barkhausen signals obtained thereby are very similar to acoustic emission signals produced in the same specimen.

Deans and Richards (1979) developped a simple and accurate method using *strain gages* applied to the centre of the back face of CT specimens and WOL T-type specimens. If the back face strain ε_{bf} measured thereby is normalized as indicated below it is only a function of a/W. The crack length ratio, a/W, is given by the calibration function

$$A^{*}(a/W) = \frac{\varepsilon_{bf}}{F} \text{ BWE} \qquad (7)$$

and Fig. 15.

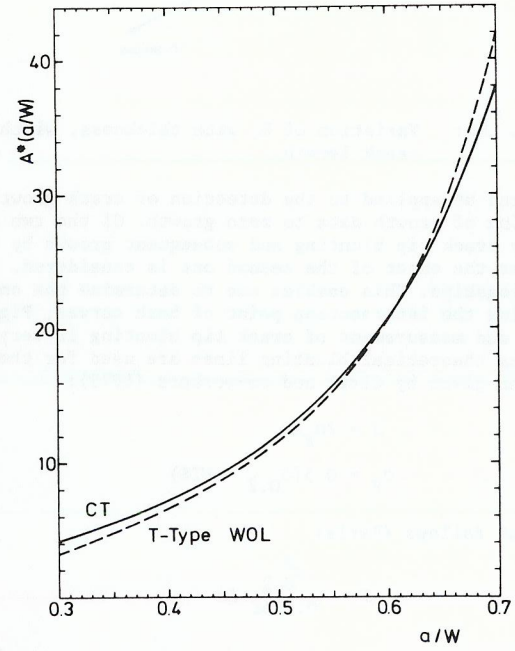

Fig. 15: Strain gage calibration curves, Den and Richards (1979).

Initiation of Crack Growth

In many cases safety philosophies are based on the initiation of crack growth rather than instabiliy. This has two reasons:

- Conservatism of the initiation values of K, J, or δ compared with the instability values.
- Instability can exhibit a large variation with size and shape whereas the initiation values of K, J, or δ are more or less constant, Fig. 16.

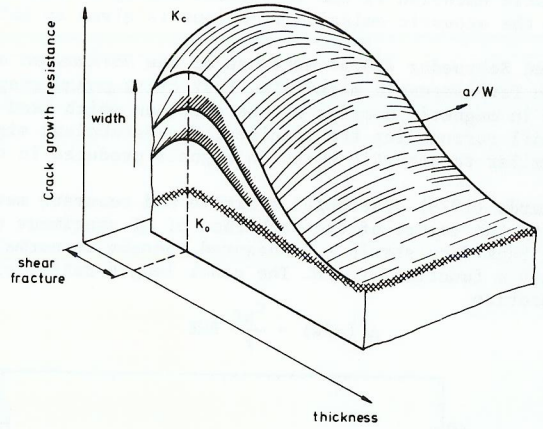

Fig. 16: Variation of K_c with thickness, width, and crack length.

Two techniques can be applied to the detection of crack growth initiation: *Back-extrapolation* of growth data to zero growth. Of the two stages of crack growth: minute growth by crack tip blunting and subsequent growth by dimple formation or similar processes the onset of the second one is considered. Both stages exhibit different relationships. This enables one to determine the onset of the second stage by constructing the intersection point of both curves, Fig. 17. Since experimental observation and measurement of crack tip blunting is very difficult due to its very small values theoretical blunting lines are used for the construction. One proposal has been given by Clark and co-workers (1979):

$$J = 2\sigma_F \Delta a \qquad (8)$$

$$\sigma_F = 0.5(\sigma_{0.2} + UTS)$$

Another one is as follows (Paris)

$$J = \frac{\sigma_{0.2}^2}{0.025E} \Delta a \qquad (9)$$

Exact quantitative measurement of a is not necessary as one is only interested in $\Delta a \rightarrow 0$.

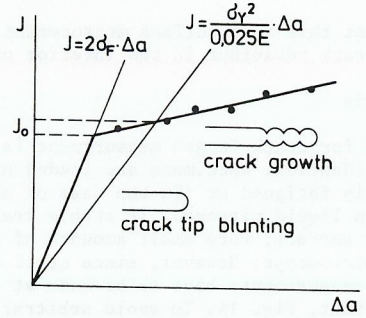

Fig. 17: Determination of Jo.

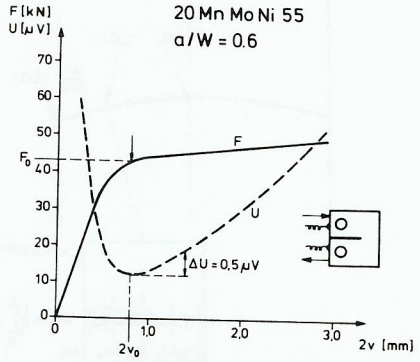

Fig. 18: Potential/COD record indicating onset of crack growth at its minimum, Blauel and Hollstein (1978).

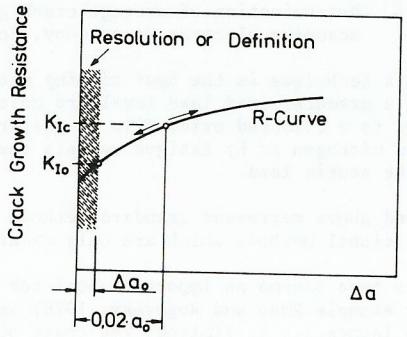

Fig. 19: Difference between K_{Ic} and K_{Io}.

A technique reported by Blauel and Hollstein (1978) allows convenient detection of the onset of stable crack growth: the *minimum occuring in the potential drop /COD-record* indicates crack growth initiation, Fig. 18.

Unfortunately only J and δ are taken at crack growth initiation, whereas the K_{Ic} value is taken at 2% crack growth, Fig. 19. Thus, these properties are not defined for the same physical event. In addition, K_{Ic} determined by the secant method can exhibit appreciable size effects, see Fig. 19. From a physical point of view a redefinition of K_{Ic} and hence a change of the procedure to determine K_{Ic} experimentally is advisable.

LOADING PARAMETERS

The loading parameters on the right hand side of Eq.(1) are related to each other in the following way (plane stress assumed):

$$K = \sigma\sqrt{\pi a}\ Y = \sqrt{GE} = \sqrt{JE} = \sqrt{m\delta E\sigma y} \qquad (10)$$

The relation between K (or G) and J or δ holds only in the case of linear elasticity, of course.

Stress Intensity and Energy Release Rate

In principle one uses known relations between K or G and other quantities, like stress or strain distribution, compliance etc. The latter quantities are determined experimentally as a function of a/W and through comparison of coefficients Y = f(a/W) is obtained.

K from local stresses or deformations

Considering the stresses σ_y on the ligament, the relation

$$\sigma_y = \frac{K}{\sqrt{2\pi x}} = \frac{\sigma\sqrt{\pi a}}{\sqrt{2\pi x}} \cdot Y \qquad (11)$$

contains all the information necessary for the determination of K. σ_y is measured for a fixed crack length as a function of x. Solving Eq.(9) for K yields

$$K = \sigma_y \sqrt{2\pi x}\,\Big|_{x\to 0} \qquad (12)$$

In Fig. 20 this procedure is outlined schematically. If this procedure is repeated as a function of crack length the calibration function

$$Y(a/W) = \frac{K}{\sigma\sqrt{\pi a}} \qquad (13)$$

can be obtained.

The local stresses can be measured using for example foil resistance strain gages, X-rays (Hellwig, 1972) or photoelastic methods (Kobayashi, 1973). An interesting aspect of photoelasticity is its applicability to three-dimensional problems (Schroedl, McGowan, and Smith, 1973). Photoelasticity studies are restricted to transparent materials. However, transparent coatings can be applied to structural materials; in this case interpretation has to consider the shear transfer between the structural materials and the coating (Kobayashi, 1978).

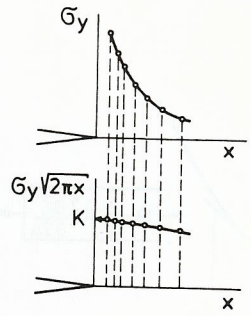

Fig. 20: Determination of K through local stress measurements.

The determination of K can be based on deformation measurements in a similar way. Methods for the measurement of displacements and strains include strain gages, optical observation of deformed grids applied to the specimen surface, the Moiré technique (Liu and Ko, 1973) and optical interference techniques. Examples are given by Kobayashi (1973, 1978).

Very convenient is the determination of the relative displacement, v, of the fracture surfaces. For plane strain the relation

$$v = \frac{4K}{E}(1-\nu^2)\sqrt{\frac{r}{2\pi}} = \sigma\sqrt{\pi a}\,\frac{4(1-\nu^2)}{E}\sqrt{\frac{r}{2\pi}} \cdot Y \qquad (14)$$

holds near the crack tip. K and Y are then determined in analogy to Eqs.(12) and (13).

Due to the restriction of the above mentioned relations to the near-tip area the measurements have to be done close to the crack tip. This implies two problems: the steep gradient near the tip requires good resolution of the method to be applied and the possibility of plastic deformations at the crack tip has to be accounted for.

G from compliance

During crack growth the energy stored in a specimen or structural part is partially released. For linear elastic behaviour the energy, U, stored per unit thickness is given by 1/2 · Fs, where F is the load and s represents the load point displacement. With the compliance C = s/F the energy released during crack growth is given by

$$G = \frac{\partial U}{\partial a} = \frac{1}{2}F^2\,\frac{\partial C}{\partial a} \qquad (15)$$

If there are two crack tips (centre cracked or double edge cracked configurations) ∂a has to be replaced by $\partial 2a$ since the partial derivative is with respect to crack area and not to crack length.

The compliance method is very simple in its principle as it requires the simultaneous measurement of load and displacement only, Fig. 21. On the other hand, this

classical method has the disadvantage that the displacements are usually small so that high accuracy is required. Differentiation of C with respect to a is an additional source of error.

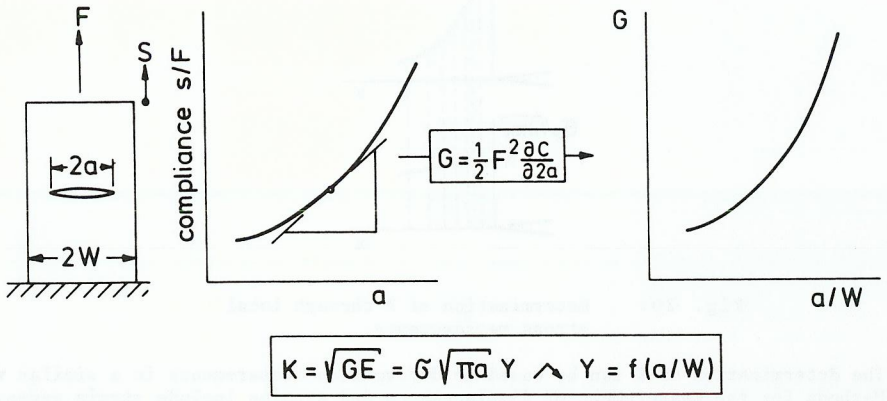

Fig. 21: Determination of Y from compliance measurements.

K from caustics

In the near-tip region of a crack in a transparent material thickness and refractive index of the material are reduced by external load. Thus this region can be regarded as a divergent lens and light passing through the specimen is deflected as shown in Fig. 22. The near-tip region appears as a dark spot or a shadow. This shadow optical effect was discovered by Manogg (1964) and further elaborated by Theocaris (1970, 1971). The method works in reflection as well as is shown in Fig. 22, if the specimen surface has been given a polish treatment. An extensive description of the method of caustics as it was named by Theocaris has been given by Beinert and Kalthoff (1979). The diameter, D, of the shadow spot is closely related to the stress intensity

$$K = MD^{-5/2}, \quad M = \frac{2\sqrt{2\pi}}{3\, f^{5/2} |c| B z_o^{5/2}} \qquad (16)$$

with f = 3.17, c = $-1.080 \cdot 10^{-10}$, B: specimen thickness, z_o: defined in Fig. 18. The relation for M and the values of f and c are valid for optically isotropic materials (like PMMA) and the case of parallel light only. Application to optically anisotropic materials and the case of reflection are described by Kalthoff (1978) and Beinert and Kalthoff (1979).

A specific advantage of the method of caustics is its applicability to the determination of dynamic stress intensities (Beinert and Kalthoff, 1979; Kalthoff, 1978), Eq. (16) can be used for the dynamic case with small errors. An exact relation can be found in the papers by the above mentioned authors. Due to dynamic effects the dynamic stress intensity, K^{dyn}, deviates significantly from the value, K^{stat}, calculated from the external load, Fig. 23. After arrest K^{dyn} exhibits oscillations with decreasing amplitude around the static value as it is also shown in Fig. 23.

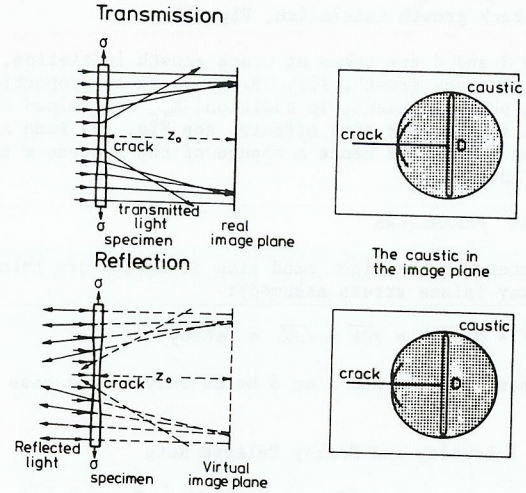

Fig. 22: The physical principle of the shadow optical method (Beinert and Kalthoff, 1979), courtesy of Beinert and Kalthoff.

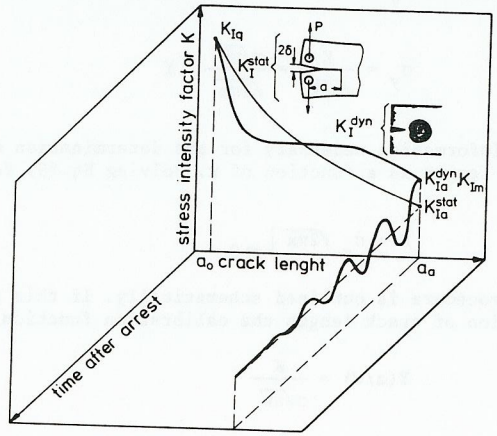

Fig. 23: Behaviour of stress intensity for running and arrested crack, Kalthoff and co-workers (1978), courtesy of Kalthoff and co-workers

K from crack growth rate

Provided that for a given material equal ΔK values yield always equal fatigue crack growth rates the latter should be independent of the geometry of the specimen (or structural part) and the crack and of the type of loading (tension, bending, single forces etc.). This can be used to calibrate the stress intensity of any configuration. The accuracy of this technique is limited through the scatter of crack growth properties.

J-Integral

J from energy

The usual way do determine J experimentally is based on the measurement of the deformation energy $\bar{U}$ put into a specimen. According to the definition

$$J = \frac{\partial \bar{U}}{\partial a} \cdot \frac{1}{B} \tag{17}$$

the energy $\bar{U}$ is measured as a function of crack length and then differentiated with respect to crack length, Fig. 24. This cumbersome procedure can be significantly improved by some sort of calibration formulae which have been developped for the most important test specimens. Landes, Walker, and Clarke (1979) propose for three point bend specimens

$$J = \frac{2\bar{U}}{B(W-a)} \qquad 0.4 < a/W < 0.8 \tag{18}$$

for the compact specimen

$$J = \frac{2\bar{U}}{B(W-a)} \cdot \frac{1+\alpha}{1+\alpha^2} \qquad 0.5 < a/W < 0.8 \tag{19}$$

$$\alpha = \sqrt{\left(\frac{2a}{W-a}\right)^2 + \frac{4a}{W-a} + 2 - \left(2\frac{a}{W-a}\right) + 1}$$

for the centre cracked tension specimen

$$J = (1-\nu^2)\frac{K^2}{E} + \frac{A}{B(W-a)} \qquad 0.4 < a/W < 0.8 \tag{20}$$

where A is the area between the test record and the secant from the origin to the point of the record under consideration.

The experimental problem here is the accurate measurement of the load point displacement. Clarke and co-workers (1976) and Clarke and co-workers (1979) have reported solutions for the CT specimen. Separate or integral knife edges are placed in the crack starter notch at the load line (= line between the midpoints of the pin holes). The situation for the bend specimens is somewhat more complicated. Usually the crosshead displacement of the testing machine is used as a measure of the specimen's deflection. To account for elastic deformations of the bend fixture and plastic deformations due to indentation of the specimen at the load application points Clarke and co-workers (1979) propose to measure a separate calibration curve on a broken half of the specimen and then to correct the original test record. This can be avoided by measuring the deflection in the way shown in Fig. 25. In Fig. 25a the deflection is measured between a pin fixed at the specimen below the loading pin and a bar attached to two pins fixed at the specimen above the two lower roller pins. An alternative solution uses two hardened plates between specimen and lower roller pins to avoid indentation, Fig. 25 b.

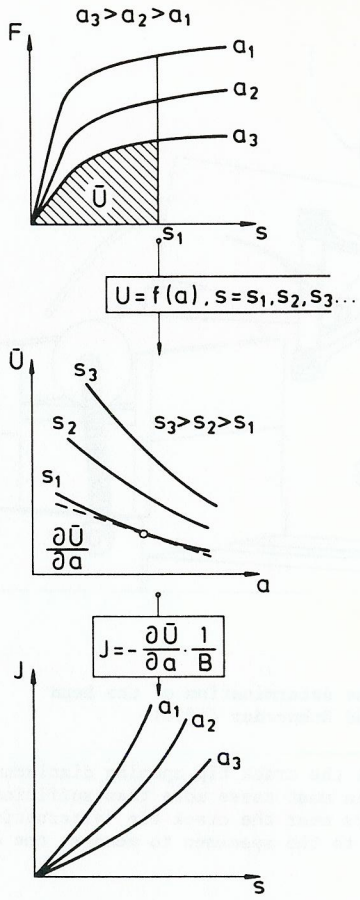

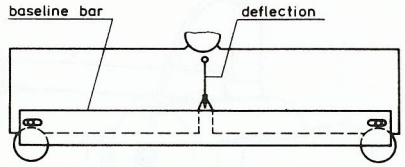

Fig. 25a: Setup for measuring the deflection of a bend specimen; Schwalbe, Hellmann and Rohwerder (1980).

Fig. 24: Determination of J via energy measurement

J from the contour integral

To the knowledge of the present author Müller and Gross (1979) were the first investigators who determined experimentally the J-integral according to its definition as a contour integral. They measured the strain field around the crack using a photoelastic coating and calculated J along rectangular paths with different lengths. They could show that J is essentially path-indepentent irrespective of the degree of plastic deformation on the ligament.

Crack Tip Opening Displacement

Surface observation

At the first glance, surface observation of the specimen near the crack tip seems

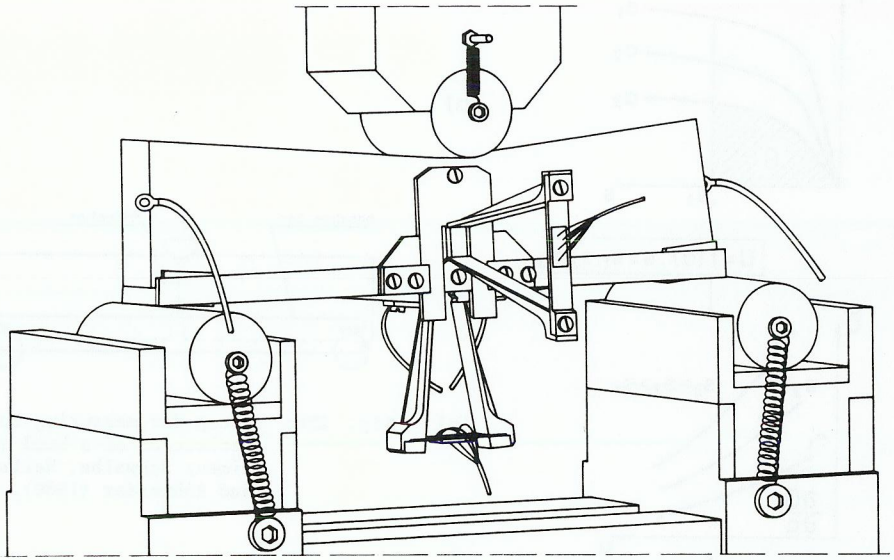

Fig. 25b: Alternative test procedure for the determination of the bend deflection; Schwalbe, Hellmann and Rohwerder (1980).

to be the most straightforward way to determine the crack tip opening displacement, δ. The resolution of an optical microscope is in most cases more than sufficient to measure the displacement of two marked points near the crack tip (alternatively a small displacement gage could be attached to the specimen to measure the displacement of these points).

This technique, however, exhibits significant disadvantages:

- The surface is not representative for the behaviour of the whole crack front (Robinson, 1973). The reasons are crack front curvature and different states of stress.
- δ exhibits a large scatter along the crack front. Surface measurement picks up a single value only. This is a poor representation of a situation which demands for averaging over measurements done at several locations.
- Another source of error is the high sensitivity of the opening displacement with respect to the location of the gage span.

Scanning electron microscopy

On the fracture surface the crack tip opening displacement creates often a steplike feature. If the specimen is tilted nearly 90° this step can be observed in profile, Fig. 26. The step hight is a measure for δ. Due to the large variation of δ on a microscopic scale, one should average over measurements taken at several locations.

It is advisable to examine both fracture surfaces to account for possible asymmetry in growth initiation. The advantage of this method is that the quantity to be measured is directly visible. However, it is extremely time consuming.

Crack Propagation Direction ⟵10µm⟶

Fig. 26: Step on the fracture surface of AlZnMgCu0.5 reflecting crack tip opening displacement; Schwalbe (1974).

Infiltration

To the knowledge of the present author Robinson (1973) was the first investigator who applied the infiltration technique to the present problem. The method has been further refined at MPI Düsseldorf (Knauf and Riedel, 1981). After the load has reached that value the crack tip deformation has to be determined for liquid silicone rubber is sucked into the crack. The hardened silicone rubber (which is removed from the fractured specimen) represents a replica of the crack tip profile which can be observed in the scanning electron microscope after sectioning in planes containing the crack tip profile.

Whereas the infiltration method gives a good impression of what happens at and near the crack tip it doesn't seem to become a routine method; since this method is very time consuming but reliable in its results it is an excellent calibration method for techniques which determine δ indirectly.

Calibration Function

The best test technique is that one which can be avoided! While direct crack tip observation is always tedious it is attractive to replace it by an indirect method which works continuously during loading and which is based on physical grounds. Such an indirect method may consist of measuring to external load or the crack mouth opening, 2v, and calculating δ via an appropriate calibration function.

By this way δ is usually determined and empirial calibration functions are used to calculate δ from 2v. Whereas these functions consider this problem primarily as a geometrical one the deformation properties of the material (yield strength, hardening behaviour) are more or less neglected.
The calibration functions:

$$\delta = \frac{8\sigma_y}{\pi E} a \ln\left\{\frac{2W}{\pi a} \arcsin\left[\sin\frac{\pi a}{2W} \sec\frac{\pi\sigma}{2\sigma_y}\right]\right\} \qquad (21)$$

(determining δ from stress, σ) and

$$\frac{\delta}{2v} = 2\,\frac{\ln A}{\dfrac{1+\sqrt{1-(1/A)^2}}{1-\sqrt{1-(1/A)^2}}}$$

$$A = \left(\frac{2}{\pi}\frac{W}{a}\right) \arcsin\left[\sin\left(\frac{\pi}{2}\frac{a}{W}\right) \sec\left(\frac{\pi}{2}\frac{\sigma}{\sigma_y}\right)\right] \qquad (22)$$

(determining δ from 2v) may be regarded as a first step towards the goal mentioned above; they are valid for centre cracked tension specimens with a finite width, 2W, and elastic-ideal plastic materials (Schwalbe, 1980a, 1980b).

REFERENCES

ASTM E647-78T(1979). Tentative Test Method for Constant-Load-Amplitude Fatique Crack Growth Rates Above 10^{-8}m/Cycle, Annual Book of ASTM Standards, Part 10, American Society for Testing and Materials, Philadelphia.

ASTM (1972). Acoustic Emission, ASTM STP 505.American Society for Testing and Materials, Philadelphia.

Aronson, G.H., and R.O. Ritchie (1979. J. of Testing and Evaluation, 7, 208-215.

Beinert, J. and J.F. Kalthoff (Manuscript completed 1979). To appear in G.C. Sih (Ed.), Mechanics of Fracture, VII.

Bhattacharya, S. and K. Schroeder (1975). J. of Testing and Evaluation, 3, 289-291.

Blauel, J.G. and T. Hollstein (1978). Arch. Eisenhüttenwes., 49,pp.587-592.

Clark, Jr.W.G. (1968). Eng. Fracture Mech., 1, 385.

Clark, G., and J.F. Knott (1975). J. Mech. Phys. Solids, 23, 265-276.

Clarke, G.A., W.R. Andrews, J. A. Begley, J.K. Donald, G.T. Embley, J.D.Landes, D.E. McCabe, and J.H. Underwood (1979). J. of Testing and Evaluation, 7, pp. 49-56.

Clarke, G.A., W.R. Andrews, P.C. Paris, and D.W. Schmidt (1976). In ASTM STP 590, pp. 27-42.

Deans, W.F., and C.E. Richards (1979). J.Testing and Evaluation, 7,147-154.

Dunegan, H., and D. Harris (1967). Ultrasonics, 7, 160.

Eftis, J., and H. Liebowitz (1972). Int. J. Fracture Mech., 4, 383-391.

Gilbey, D.M. and S. Pearson (1966). RAE TR 66402, Royal Aircraft Establishment, Farnborough.

Greenberg, H.D., E.T. Wessel, W.G. Clark, Jr. and W.H. Pryle (1969). Westinghouse Scientific Paper 69 - 1D9 - MEMTL-P1.

Hartbower, D.E., C.F. Morais, W.G. Reuter, and P.D. Crimmins (1973). Eng. Fracture Mech., 5, 765-789.

Hellmann, D. (1980). Unpublished results.

Hellwig, G., (1972). Doctoral Dissertaion, Karlsruhe.

Johnson, H.H. (1965). Mat. Res. and Standards, 5, 442-445.

Kalthoff, J. (1978). Fortschr.-Ber. VDI-Z., Reihe 18, Nr. 4, VDI-Verlag, Düsseldf.

Kalthoff, J. J. Beinert, S. Winkler, and W. Klemm (1978). Paper presented at ASTM -E24 Symposium on Crack Arrest Methodology and Applications, Philadelphia.

Klima, S.J., D.M. Fisher, and R.J. Buzzard (1976). J. of Testing and Evaluation, 4, 397-404.

Knauf, G., and H. Riedel (1981). The 5th International Conference on Fracture, Cannes.

Kobayashi, A.S. (1978). In N. Perrone, H. Liebowitz, D. Mulville, and W. Pilkey (Eds.), Fracture Mechanics, University Press of Virginia, Charlottesville, pp. 481-496.

Kobayashi, A.S. (1973). Experimental Techniques in Fracture Mechanics, Society for Experimental Stress Analysis, Westport.

Landes, J.D., H. Walker, and G.A. Clarke (1979). In ASTM STP 668, pp. 266-287.

Liu, H.W., and J.S. Ko (1973). In A.S. Kobayashi (Ed.), Experimental Techniques in Fracture Mechanics, Society for Experimental Stress Analysis, Westport.

Manogg, O.(1964). Ph. D. Thesis, Freiburg.

Munz, D. (1976). Z. Werkstofftechnik, 7, 111.

Müller, Th. and D. Gross (1979). Paper presented at the eleventh meeting of the"Arbeitskreis Bruchvorgänge im DVM", Stuttgart.

Paris, P.C. (refered to in Munz, 1976).

Ritchie, R.O., and K.J. Bathe (1979). Int. J. of Fracture, 15, 47-55.

Robinson, J.N. (1973). Ph.D.Thesis, University of California, Los Angeles.

Rooke, D.P. (1967). RAE TR 67160, Royal Aircraft Establishment, Farnborough.

Rose, J.L., and A.J. Rogovsky (1978). In N. Perrone, H. Liiebowitz, D. Mulville, and W. Pilkey (Eds.), Fracture Mechanics, University Press of Virginia, Charlottesville, pp. 455-469.

Russenberger, M.E. (1979). Materialprüfung, 21, 319-321.

Schroedl, M.A., J.J. McGowan, and C.W. Smith (1973). Report VPI-E-73-34, Virginia Polytechnic Institute and State University, pp. 111-165.

Saxena, A., and S.J. Hudak, Jr. (1978). Int. J. Fracture, 14, 453-468.

Schwalbe, K.-H. (1972). Int. J. of Fracture Mech., 8, 456-457.

Schwalbe, K.-H. (1974). Eng. Fracture Mech., 6, pp. 415-434.

Schwalbe, K.-H. (1977a). Eng. Fracture Mech., 9, 547-556.

Schwalbe, K.-H. (1977b). Eng. Fracture Mech., 9, 557-583.

Schwalbe, K.-H. (1979). Eng. Fracture Mech., 11, 331-342.

Schwalbe, K.-H. (1980). Bruchmechanik metallischer Werkstoffe. Carl-Hanser-Verlag, München.

Schwalbe, K.-H. (1980a). ASTM STP 700.

Schwalbe, K.-H. (1980b). Unpublished results.

Schwalbe, K.-H., and D. Hellmann (Submitted for publication).

Schwalbe, K.-H., D. Hellmann, and G. Rohwerder (1980). In preparation.

Schwalbe, K.-H., and W. Setz (Submitted for publication).

Schwalbe, K.-H., W. Setz, L. Schwarmann, W. Geier, C. Wheeler, D. Rooke, A.U.de Koning, and J. Eastabrook. Fortschr. Ber. VDI-Z., Reihe 18, Nr. 9.

Sullivan, A.M. (1975). NRL Report 7941.

Sullivan, A.M., and J. Stoop (1974). NRL Report 7674.

Theocaris, P.S. (1970). J. Appl. Mech., 37, pp. 409.

Theocaris, P.S. (1971). Materialprüfung, 13, pp. 264-269.